Supplementary Information

Influence of structure and solubility of chain transfer agents on the RAFT control of dispersion polymerisation in $scCO_2$

Ana A. C. Pacheco,[a] *Arnaldo F. da Silva Filho,[a] Kristoffer Kortsen,[a] Magnus W. D. Hanson-Heine,[a] Vincenzo Taresco,[a] Jonathan D. Hirst,[a] Franck D'Agosto,[b]* Muriel Lansalot,[b]* and Steven M. Howdle [a]**

[a] University of Nottingham, Chemistry Department, University Park, Nottingham, NG7 2RD, England; [b] Univ Lyon, Université Claude Bernard Lyon 1, CPE Lyon, CNRS, UMR 5265, Chemistry, Catalysis, Polymers and Processes (C2P2), 43 Bd du 11 Novembre 1918, 69616 Villeurbanne, France.

Corresponding Author

Franck D'Agosto,[b] Muriel Lansalot [b]* and Steven M. Howdle [a]**

a. University of Nottingham, University Park, Nottingham, NG7 2RD, England. steve.howdle@nottingham.ac.uk
b. Univ Lyon, Université Claude Bernard Lyon 1, CPE Lyon, CNRS, UMR 5265, Chemistry, Catalysis, Polymers and Processes (C2P2), 43 Bd du 11 Novembre 1918, 69616 Villeurbanne, France. franck.dagosto@univ-lyon1.fr; muriel.lansalot@univ-lyon1.fr

(A) DDMAT (B) CPDT

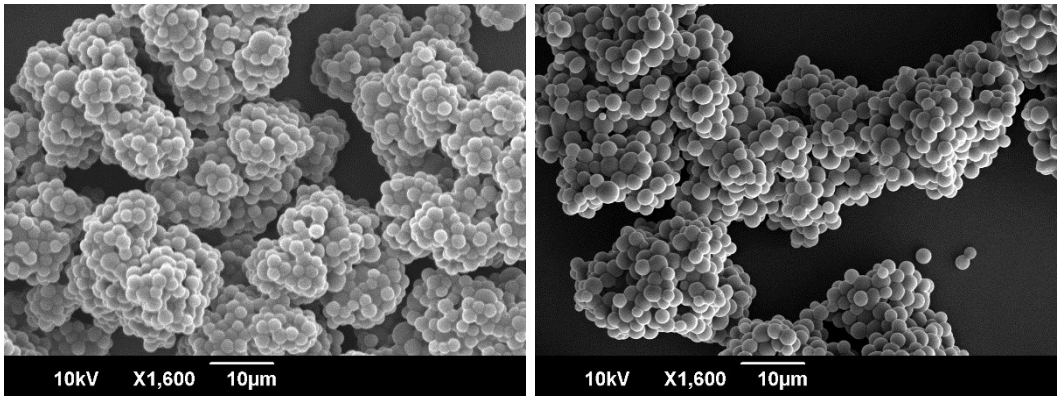

(C) CPAB

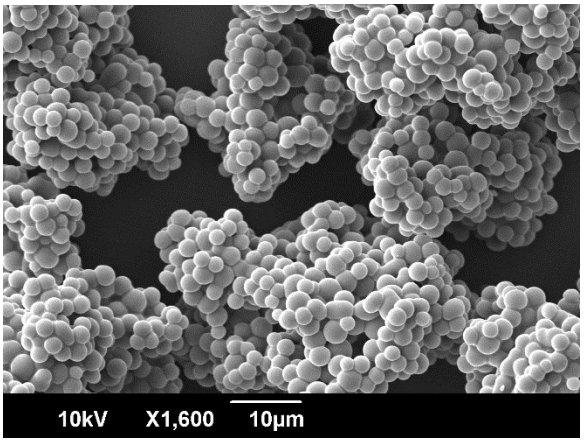

Figure S1 *SEM images of PMMA synthesised in $scCO_2$ via RAFT dispersion polymerisation with (A) DDMAT, average diameter = 2.11 μm and C_v = 17%; (B) CPDT, average diameter = 2.26 μm and C_v = 20.5%; (C) CPAB, average diameter = 2.43 μm and C_v = 15%.*

Table S1 *Particle size analysis via SEM of PMMA synthesised in $scCO_2$ with different CTAs. The average particle size, presented as an average of 100 particles measurements, and the coefficient of variance, which is calculated by the ratio of the standard deviation (σ) by the mean particle diameter as by the equation* $C_v = \sigma/D_n \times 100$, are presented. *Results are an average from all reactions performed with the given CTA.*

CTA	particle size (μm)	C_v (%)
DDMAT	2.11	23.24
CPAB	2.67	18.15
CPDT	2.57	17.07

Table S2 *Data from a triplicate repeat of the kinetic study of RAFT polymerisation of MMA with DDMAT using the high pressure sampling device.*

Reaction 1				
Time (h)	conv (%) [1]	$M_{n,th}$ (kg mol^{-1}) [3]	M_n (kg mol^{-1}) [2]	$Đ$ [2]
4	13.0	7.8	13.8	1.62
6	30.1	17.9	20.7	1.36
8	47.4	28.2	29.9	1.30
20	91.1	54.2	55.6	1.39
24	96.8	57.6	62.1	1.27
Reaction 2				
Time (h)	conv (%) [1]	$M_{n,th}$ (kg mol^{-1}) [3]	M_n (kg mol^{-1}) [2]	$Đ$ [2]
2	6.5	3.9	10.1	1.36
4	17.3	10.3	15.3	1.32
6	35.4	20.9	21.2	1.30
18	91.4	54.0	54.8	1.34
20	96.8	57.2	56.4	1.33
24	98.4	58.2	62.2	1.29
Reaction 3				
Time (h)	conv (%) [1]	$M_{n,th}$ (kg mol^{-1}) [3]	M_n (kg mol^{-1}) [2]	$Đ$ [2]
2	5.7	3.3	10.3	1.35
4	15.3	8.9	14.3	1.36
6	31.0	18.2	20.6	1.29
8	46.5	27.2	27.2	1.28
10	60.3	35.3	37.6	1.29
12	83.3	48.8	47.7	1.28
24	98.6	57.8	58.8	1.28

[1] Conversion calculated from ^{1}H NMR. [2] $Đ$ and M_n obtained by THF-SEC with RI detector against PMMA standards, M_n given in kg mol^{-1}. [3] Theoretical M_n calculated relative to CTA and monomer concentration and given in kg mol^{-1}.

(A)

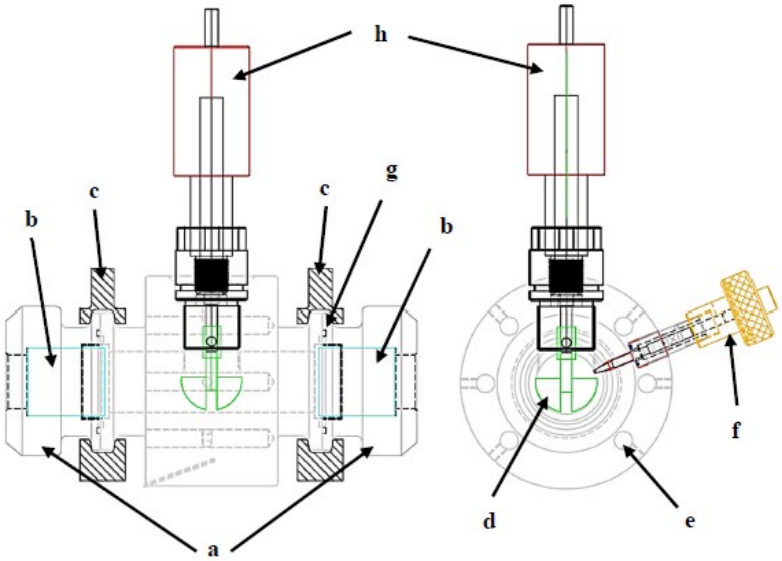

(B)

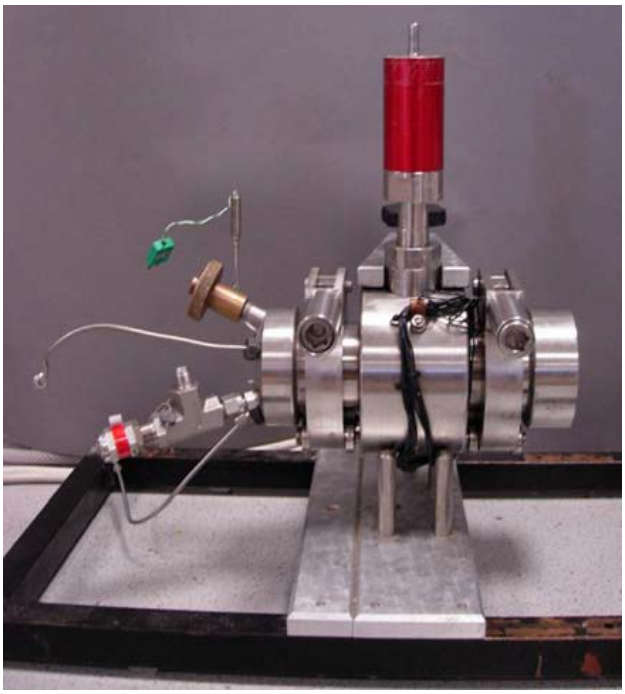

Figure S2 *Side (left) and front (right) schematic (A) and photograph of the static view cell autoclave (B). The view cell parts consist of a) view ports, b) sapphire windows, c) sealing clamps, d) stirrer blade, e) heating cartridges, f) safety key and needle, g) EPDM O-ring and h) magnetically coupled overhead stirrer, as seen in the schematic (A).*

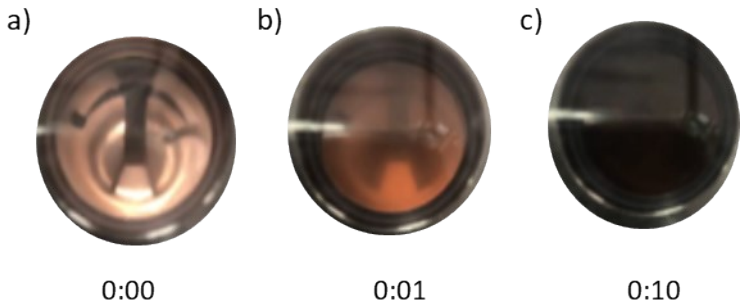

Figure S3 *View cell photographs showing the phase behaviour of the free-radical dispersion polymerisation of MMA in $scCO_2$. a) Prior to reaction onset the reactants are all soluble in $scCO_2$ and one can see through the view-cell; b) After 1 minute of reaction, turbidity is noticeable; c) At 10 minutes, the passage of light is completely blocked. Reaction set at 275 bar, 65 °C, MMA (0.1 mol), AIBN (0.08 mmol) and PDMS-MA (10 kg mol^{-1}, at 5 wt% relative to MMA).*

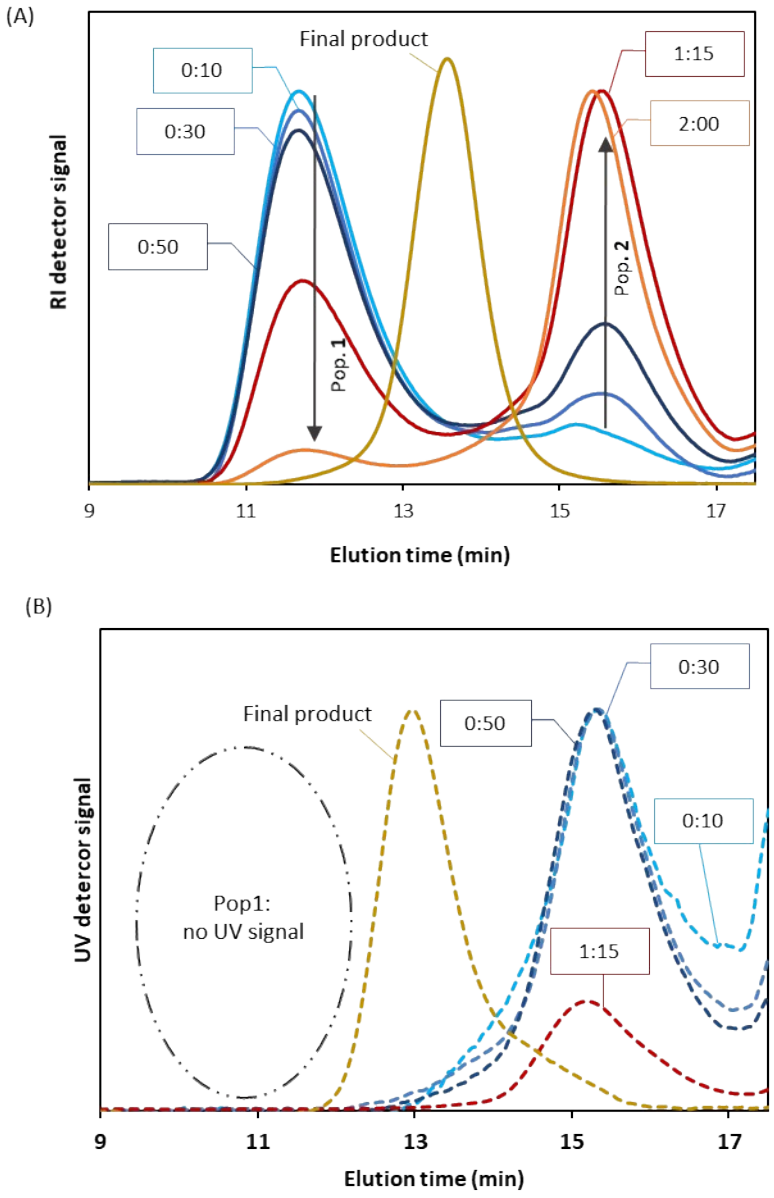

Figure S4 *Early stage study of RAFT dispersion polymerisation of MMA in $scCO_2$ with DDMAT, showing the THF-SEC study of aliquots from the reaction sampling device against the RI detector (A) and the UV detector (B). It is noticeable that population 1 does not present a UV signal, while population 2 shows UV absorption at 300 nm. Results in (A) are normalised while the UV response is not normalised.*

Table S3 *Data from triplicate repeats of the kinetic study of RAFT polymerisation of MMA with CPAB using the high pressure sampling device.*

Reaction 1				
Time (h)	conv (%) [1]	$M_{n,th}$ (kg mol^{-1}) [3]	M_n (kg mol^{-1}) [2]	$Đ$ [2]
2.3	5.6	3.4	2.3	1.10
4.	11.5	7.0	4.0	1.14
6.	22.5	13.6	8.5	1.21
20	92.7	56.3	79.2	1.53
22	98.6	60.0	80.8	1.39
24	98.9	60.1	81.9	1.43
Reaction 2				
Time (h)	conv (%) [1]	$M_{n,th}$ (kg mol^{-1}) [3]	M_n (kg mol^{-1}) [2]	$Đ$ [2]
2	8.2	4.9	2.6	1.08
4	9.9	5.9	4.9	1.13
6	17.4	10.4	10.7	1.11
7.8	28.1	16.8	17.6	1.15
22	98.3	58.9	72.9	1.50
24.5	98.9	59.2	73.8	1.48
Reaction 3				
Time (h)	conv (%) [1]	$M_{n,th}$ (kg mol^{-1}) [3]	M_n (kg mol^{-1}) [2]	$Đ$ [2]
2.00	6.5	3.9	2.2	1.15
4.00	11.5	6.9	3.7	1.33
6.00	27.0	16.2	10.1	1.16
8.33	28.0	16.8	19.9	1.19
10.00	43.8	26.2	30.1	1.25
12.00	57.4	34.4	42.1	1.43
24.00	94.9	56.8	84.0	1.51

[1] Conversion calculated from ^{1}H NMR. [2] $Đ$ and M_n obtained by THF-SEC with RI detector against PMMA standards, M_n given in kg mol^{-1}. [3] Theoretical M_n calculated relative to CTA and monomer concentration and given in kg mol^{-1}.

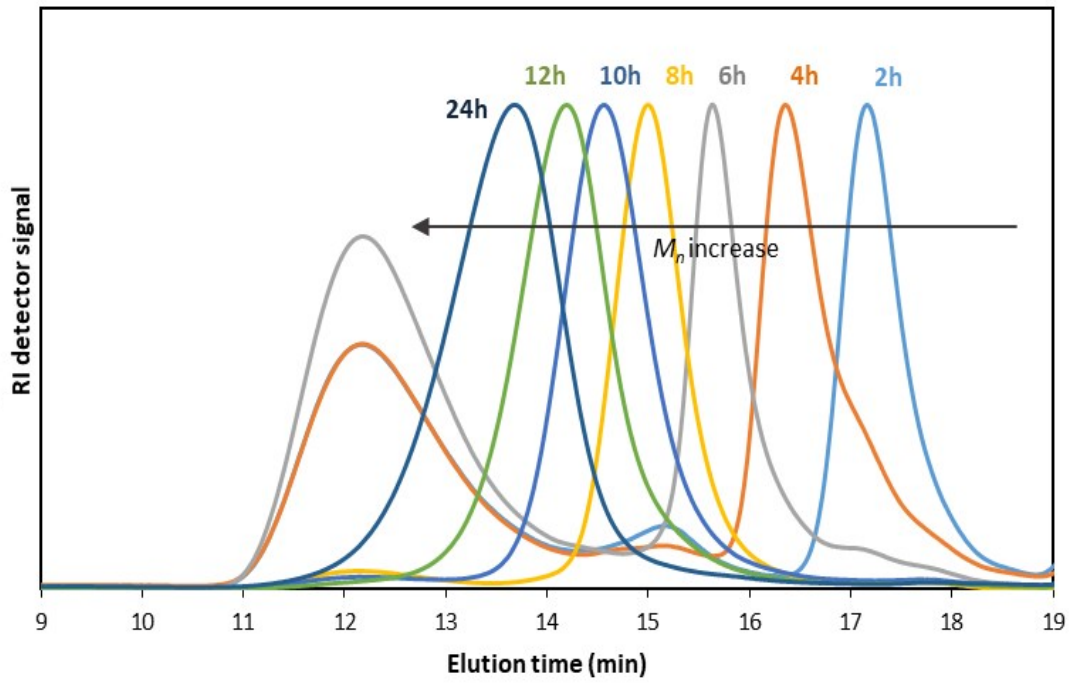

Figure S5 *Normalised SEC traces showing the molecular weight distributions of the samples withdrawn for the $scCO_2$ dispersion polymerisation of MMA with CPAB.*

(A)

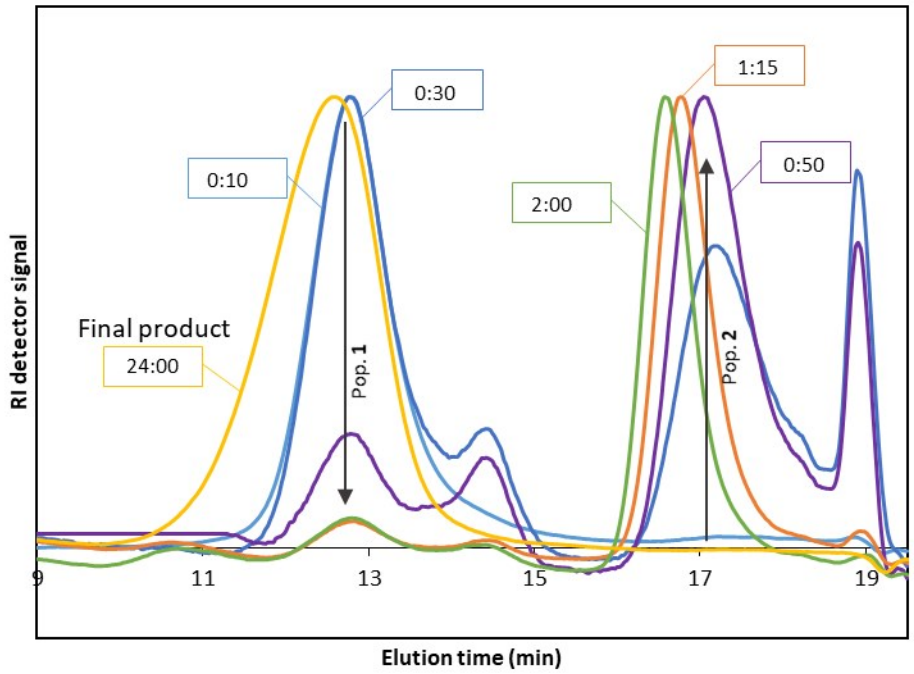

(B)

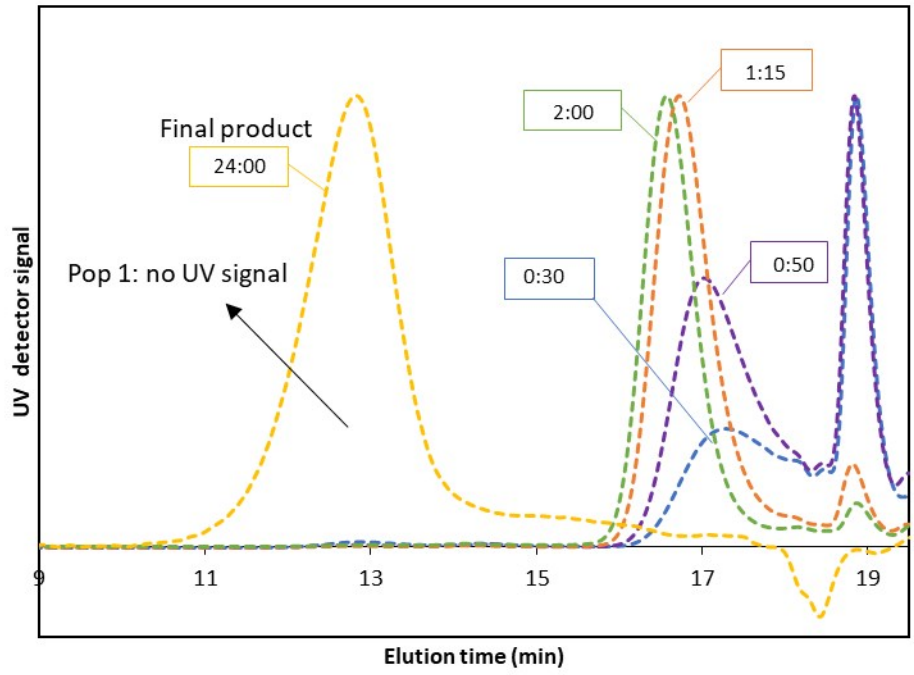

Figure S6 *Early stage study of RAFT dispersions polymerisation of MMA in $scCO_2$ with CPAB, showing the THF-SEC SEC study of aliquots from reaction on sampling device against the RI detector (A) and the UV detector (B). It is noticeable that population 1 does not present UV signal, while population 2 show UV absorption at 300 nm. Results in (A) are normalised while the UV response is not normalised.*

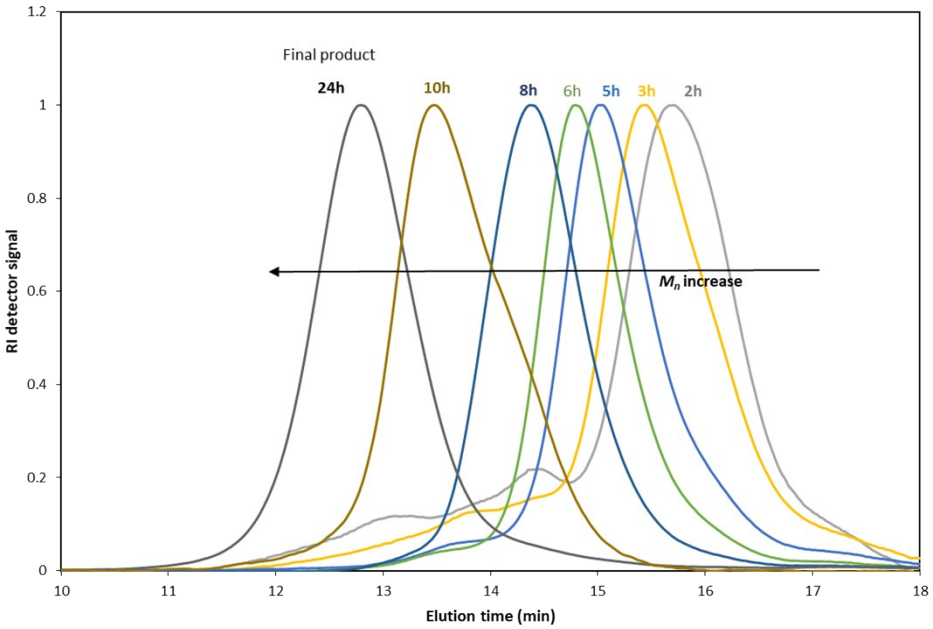

Figure S7 *Normalised SEC traces showing the molecular weight distributions of the samples withdrawn for the scCO$_2$ dispersion polymerisation of MMA with CPDT. Data retrieved from our previous publication.[1]*

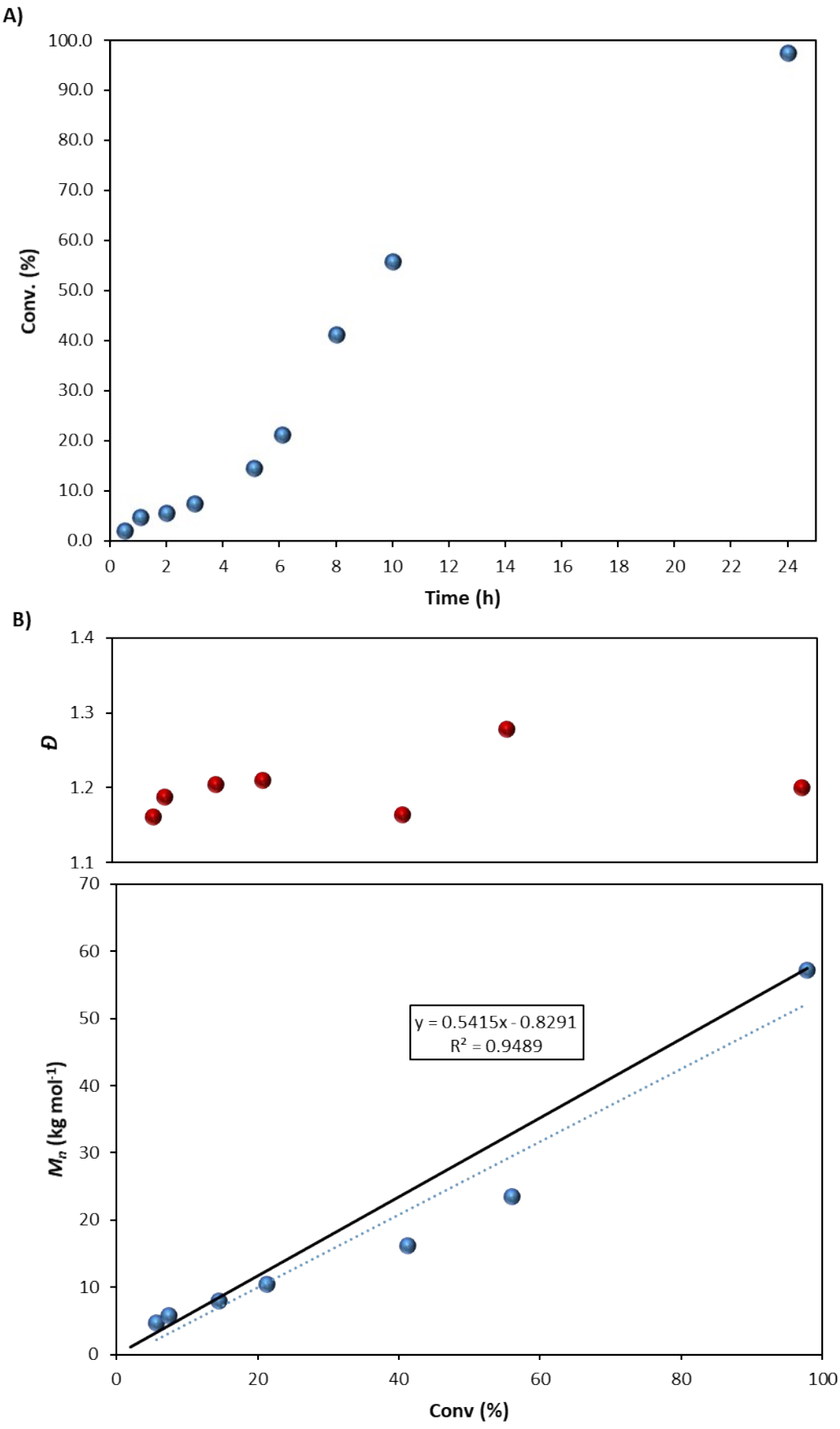

Figure S8 *Dispersion polymerisation of MMA in scCO$_2$ using CPDT as CTA as retrieved from our previous publication.[1] (A) Evolution of MMA conversion* versus *time. (B) Evolution of M$_n$ (blue) and Đ (red)* versus *conversion; solid trend line is the*

theoretical M_n and dashed trend line is the linear fitting of experimental data. (Molar ratio CPDT/AIBN 2:1, 65 °C, 275 bar, 300 rpm stirring rate, 5 wt% of PDMS-MA as stabiliser (based on MMA)).

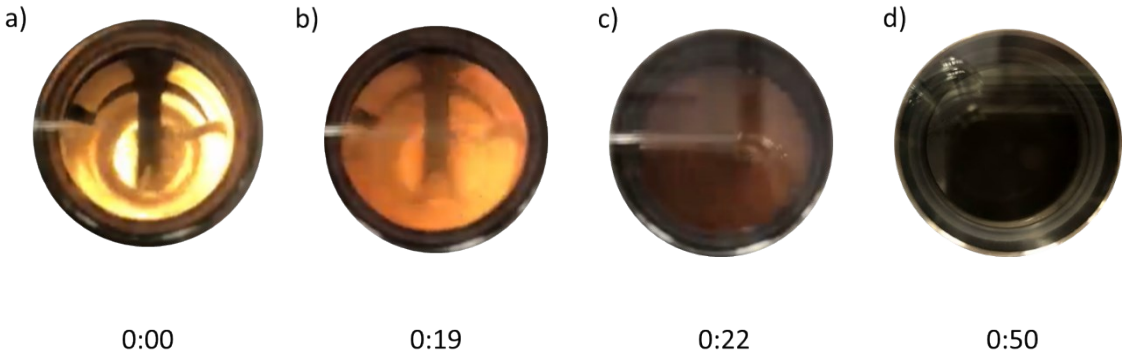

Figure S9 *View cell photographs showing the phase behaviour of the RAFT dispersion polymerisation of MMA in $scCO_2$ with CPDT. a) Prior to reaction onset the reactants are all soluble in $scCO_2$ and one can see through the view-cell; b) After 19 minutes, turbidity is noticeable; c) At 22 minutes, turbidity increases; d) At 50 minutes, the passage of light is completely blocked. Reaction set at 275 bar, 65 °C, MMA (0.1 mol), AIBN (0.08 mmol) and PDMS-MA (10 kg mol^{-1}, at 5 wt% relative to MMA).*

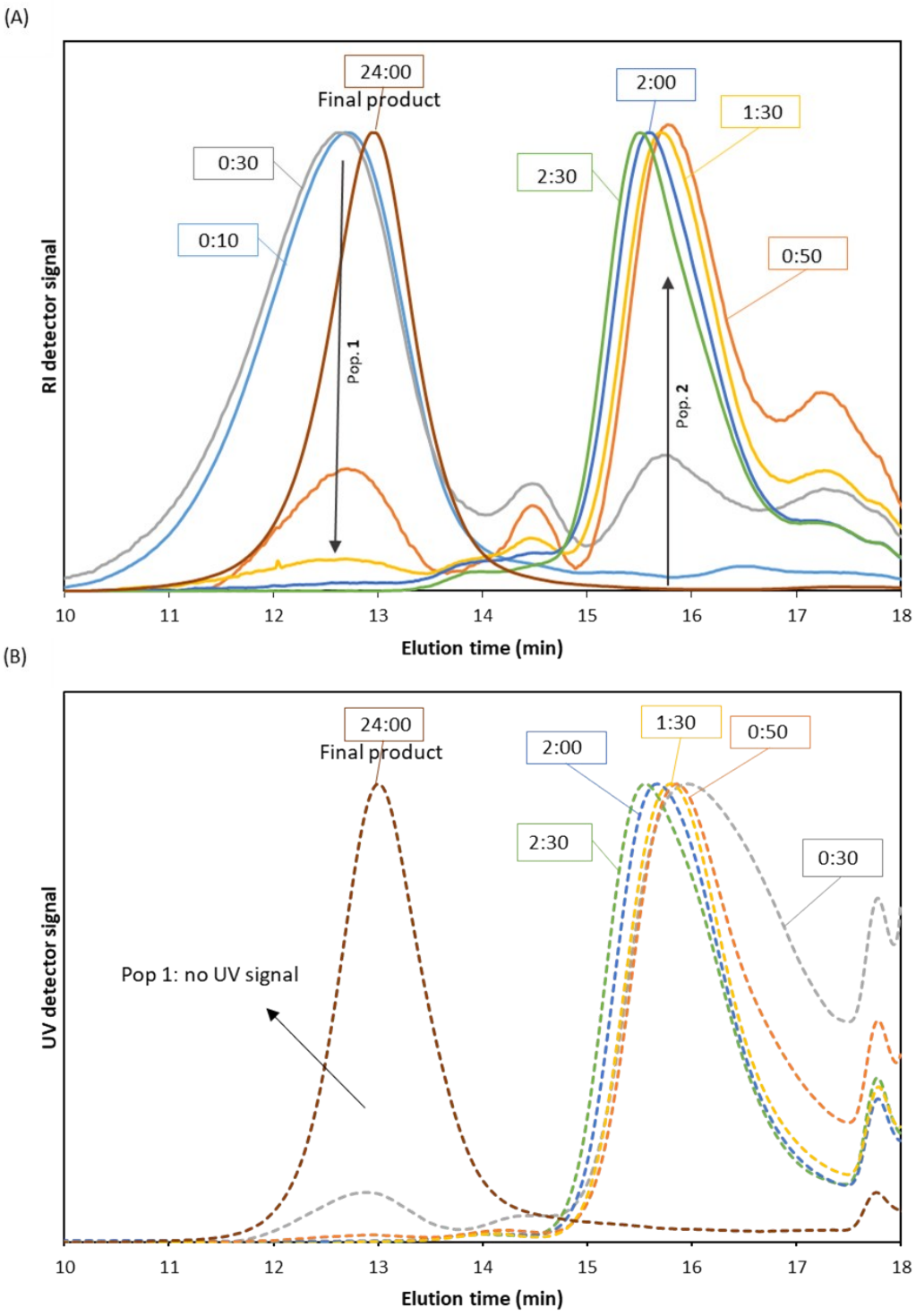

Figure S10 *Early stage study of RAFT dispersion in $scCO_2$ with CPDT, showing the THF SEC study of aliquots from reaction on sampling device against the dRI detector (A) and the UV detector (B). It is noticeable that population 1 does not present UV signal, while population 2 show UV absorption at 300 nm. Results in (A) are normalised while the UV response is not normalised.*

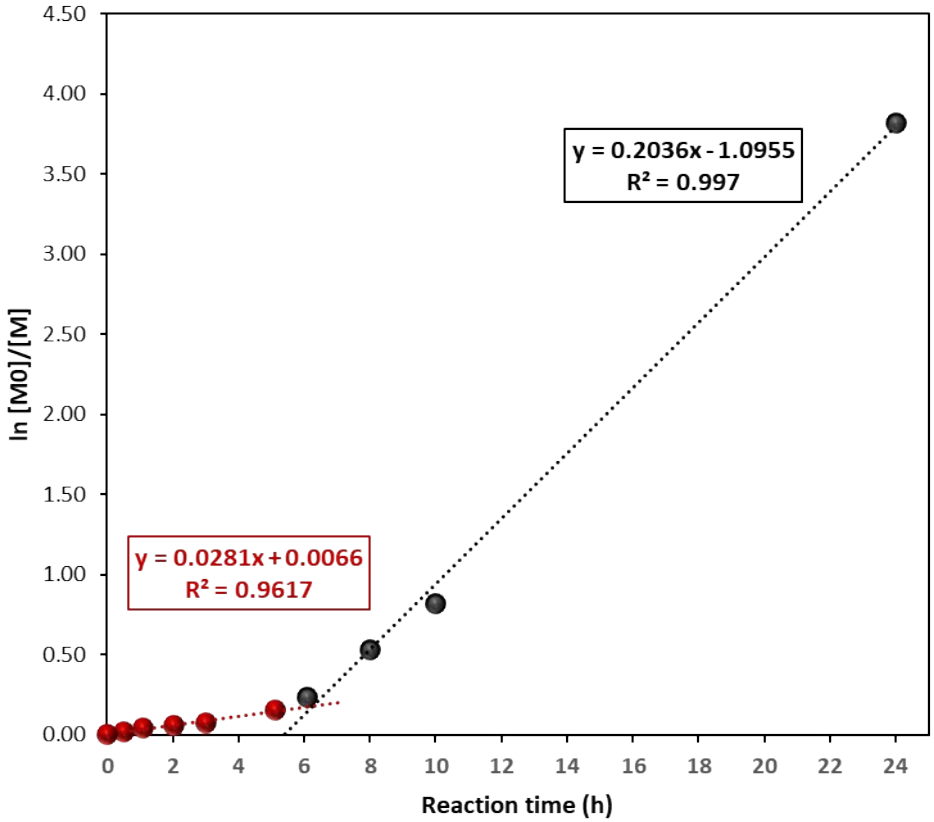

FigureS11 *Pseudo-first-order kinetic plot of monomer conversion as a function of reaction time for the dispersion polymerisation of MMA in scCO_2 with CPDT, highlighting two distinct regimes (red and grey data points and trend lines).*

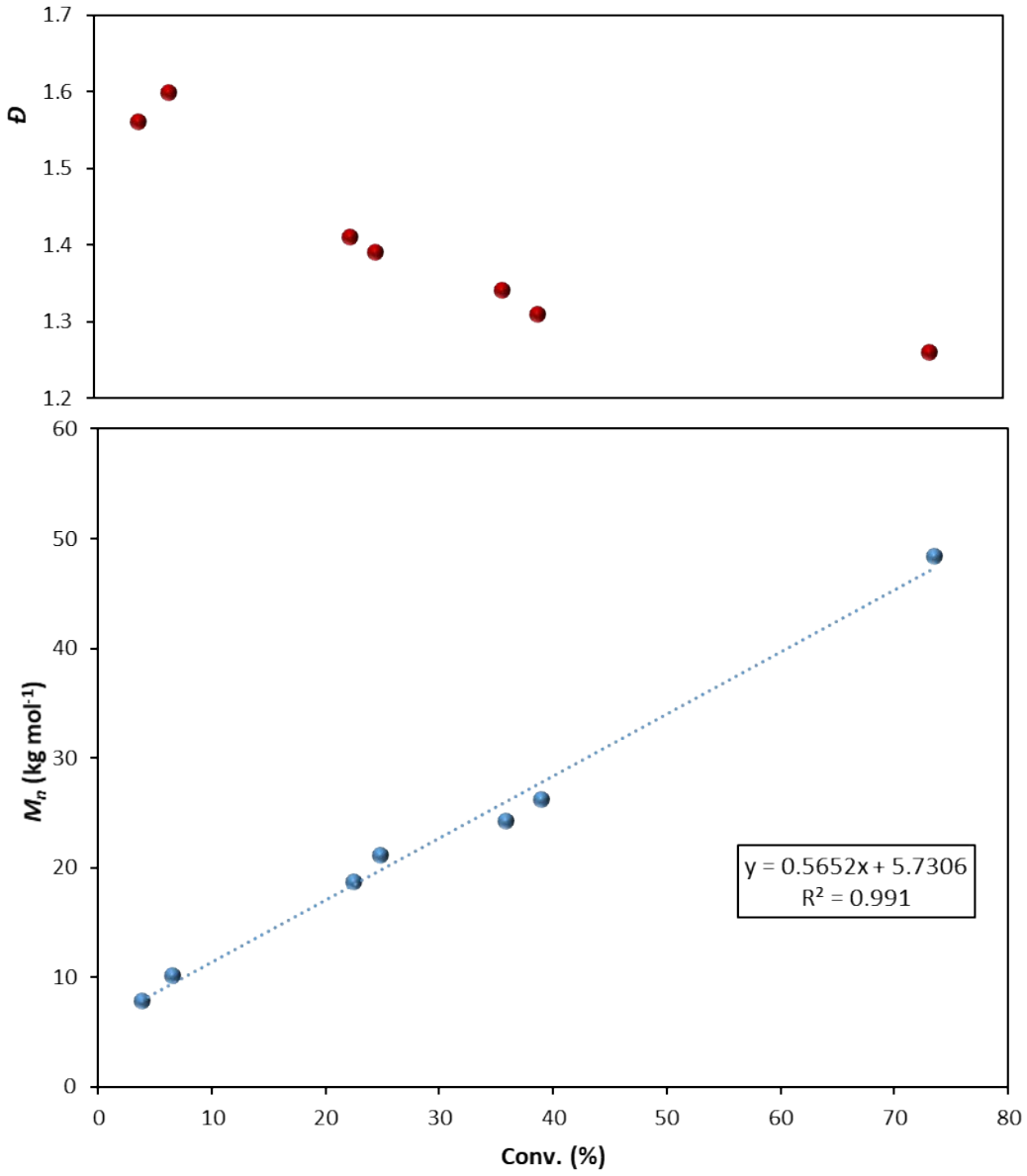

Figure S12 *Toluene solution polymerisation of MMA using CPDT as CTA. (A) Evolution of MMA conversion* versus *time. (B) Evolution of* M_n *(blue) and Đ (red)* versus *conversion; the dashed trend line is the linear fitting of experimental data. (Molar ratio CPDT/AIBN 5:1, 65 °C, in toluene).*

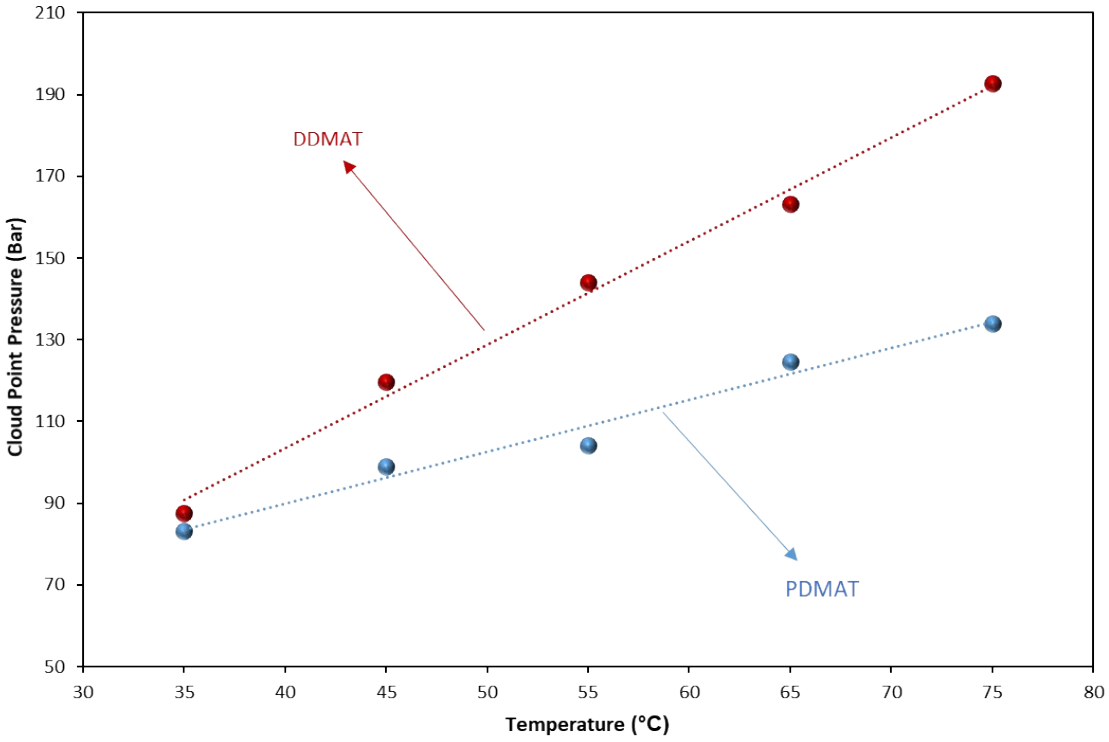

Figure S13 *Cloud point study of CTAs in variable volume view cell for DDMAT (blue) vs PDMAT (red). The cloud point indicates the minimal pressure needed for solubilising the solute at a given temperature; as the cloud point for PDMAT is lower than for DDMAT at all pressures, PDMAT is more soluble in scCO_2 that DDMAT. (Cloud point study performed with 20 g of CO_2, 3.33 g of MMA and 6.30.10^{-5} mol of CTA).*

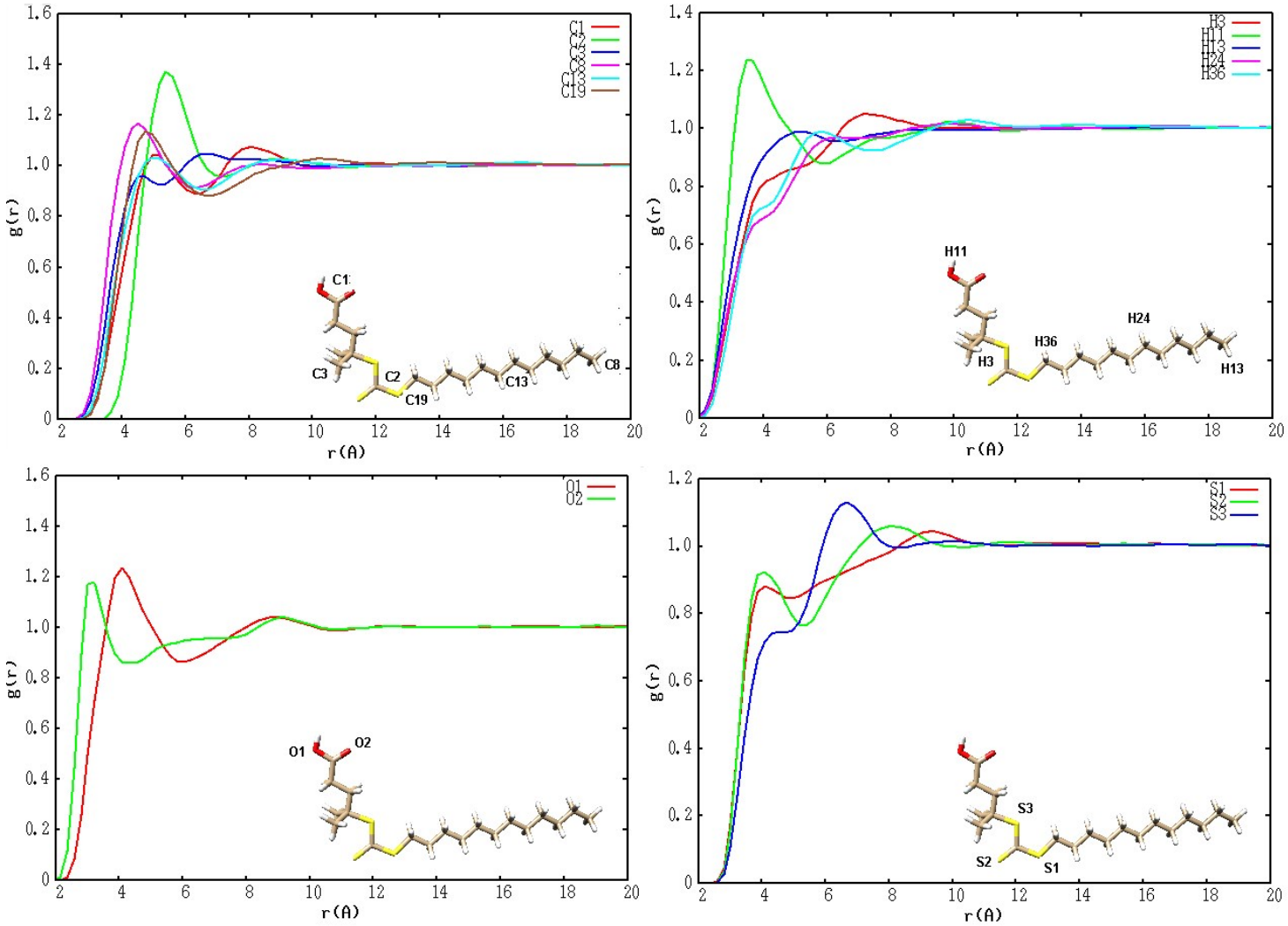

Figure S14 *Radial distribution functions showing the functional groups interactions with $scCO_2$, gij(r) (i = O1 - - -, O2 .... or N1 ___ and j = carbon atoms of CO_2) vs. interatomic distances. From top left to bottom right: Carbon atoms of DDMAT; Hydrogen atoms of DDMAT; Oxygen atoms of DDMAT; Oxygen atoms of DDMAT; and Sulfur atom of DDMAT.*

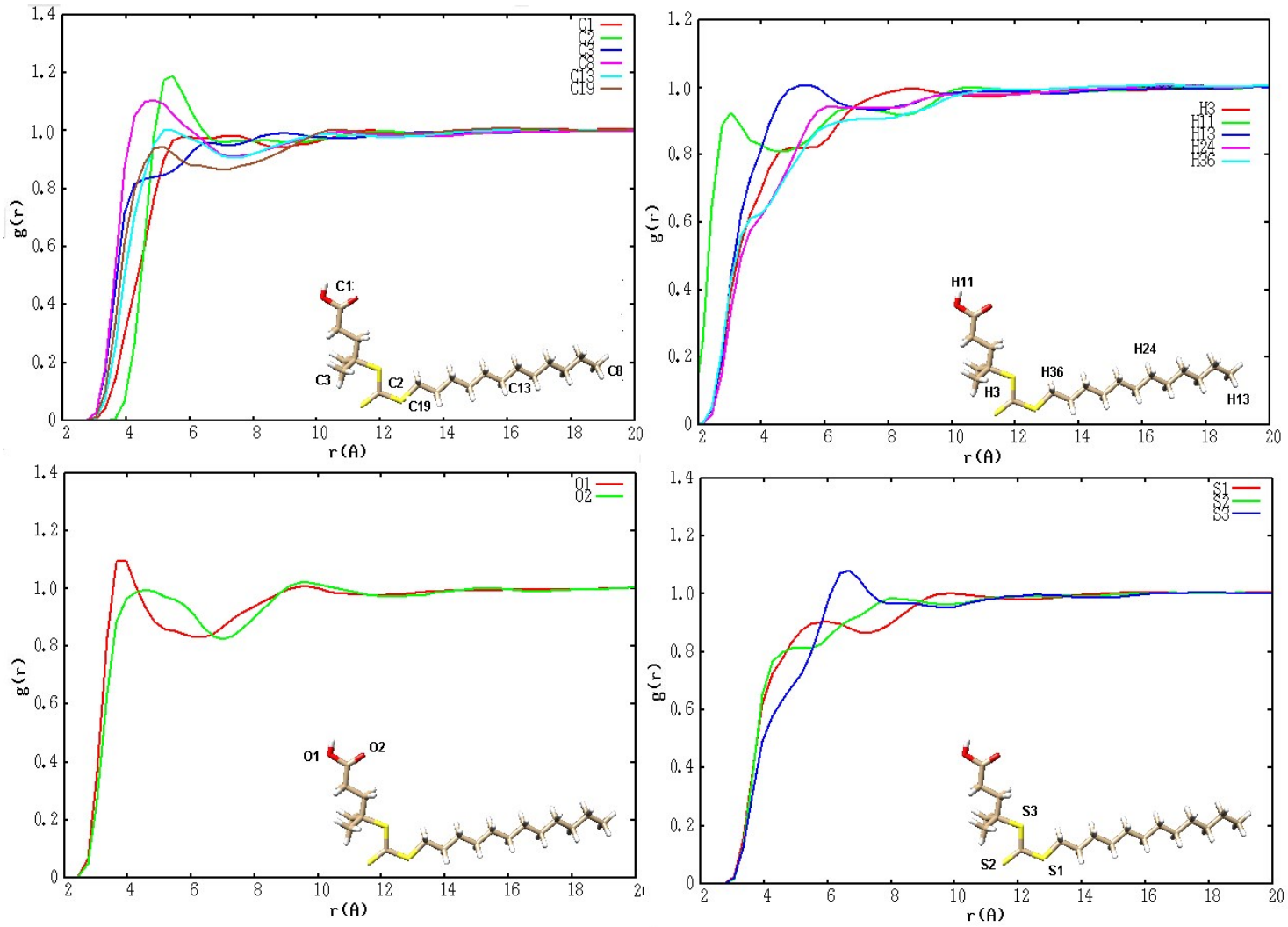

Figure S15 *Radial distribution functions showing the functional groups interactions with toluene, gij(r) (i = O1 - - -, O2 .... or N1 ___ and j = carbon atoms of toluene) vs. interatomic distances. From top left to bottom right: Carbon atoms of DDMAT; Hydrogen atoms of DDMAT; Oxygen atoms of DDMAT; Oxygen atoms of DDMAT; and Sulfur atoms of DDMAT.*

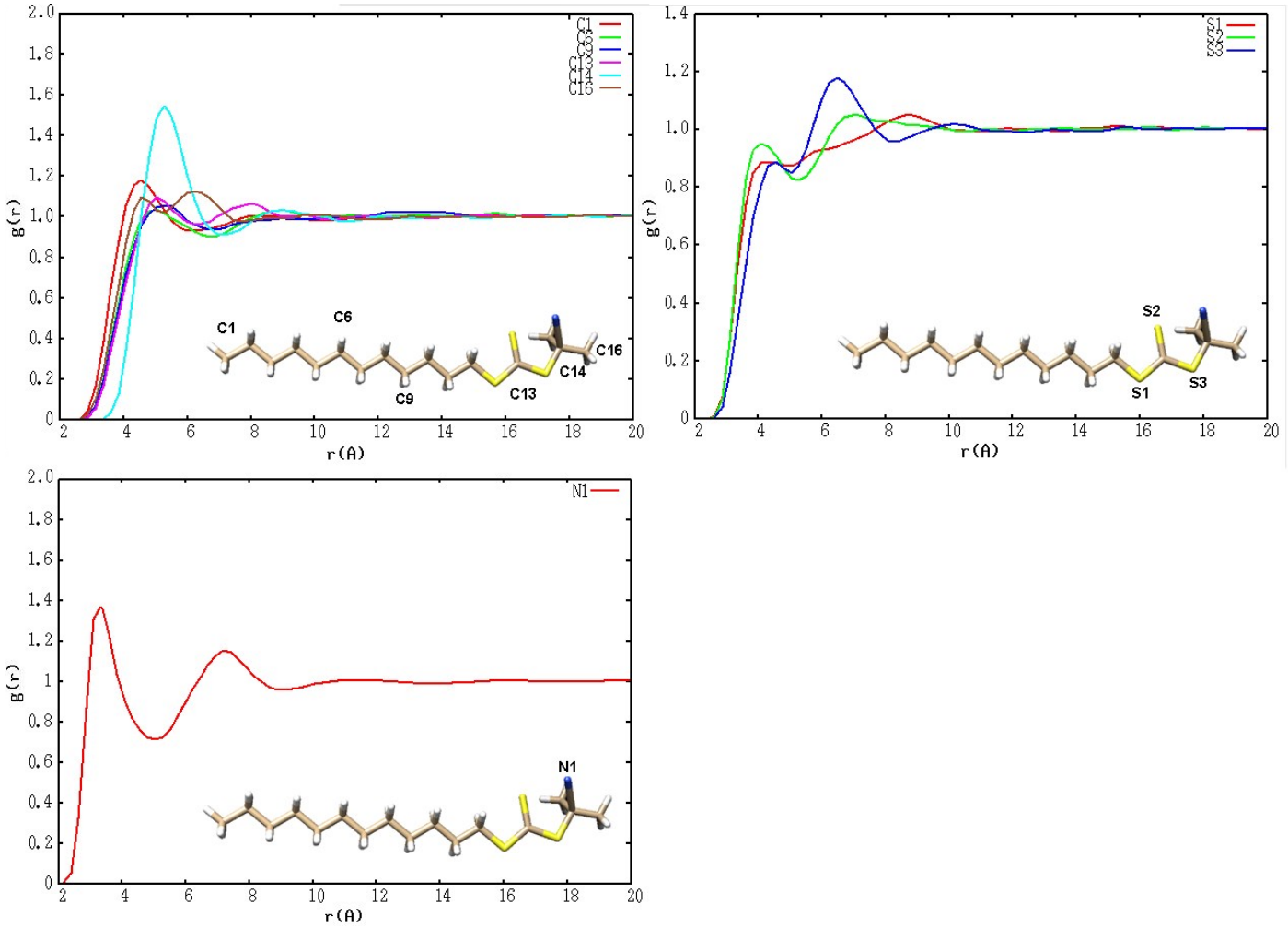

Figure S16 *Radial distribution functions showing the functional groups interactions with $scCO_2$, gij(r) (i = O1 - - -, O2 .... or N1 ___ and j = carbon atoms of CO_2) vs. interatomic distances. From top left to bottom left: Carbon atoms of CPDT; Sulfur atoms of CPDT; Oxygen atoms of CPDT; Nitrogen atom of CPDT.*

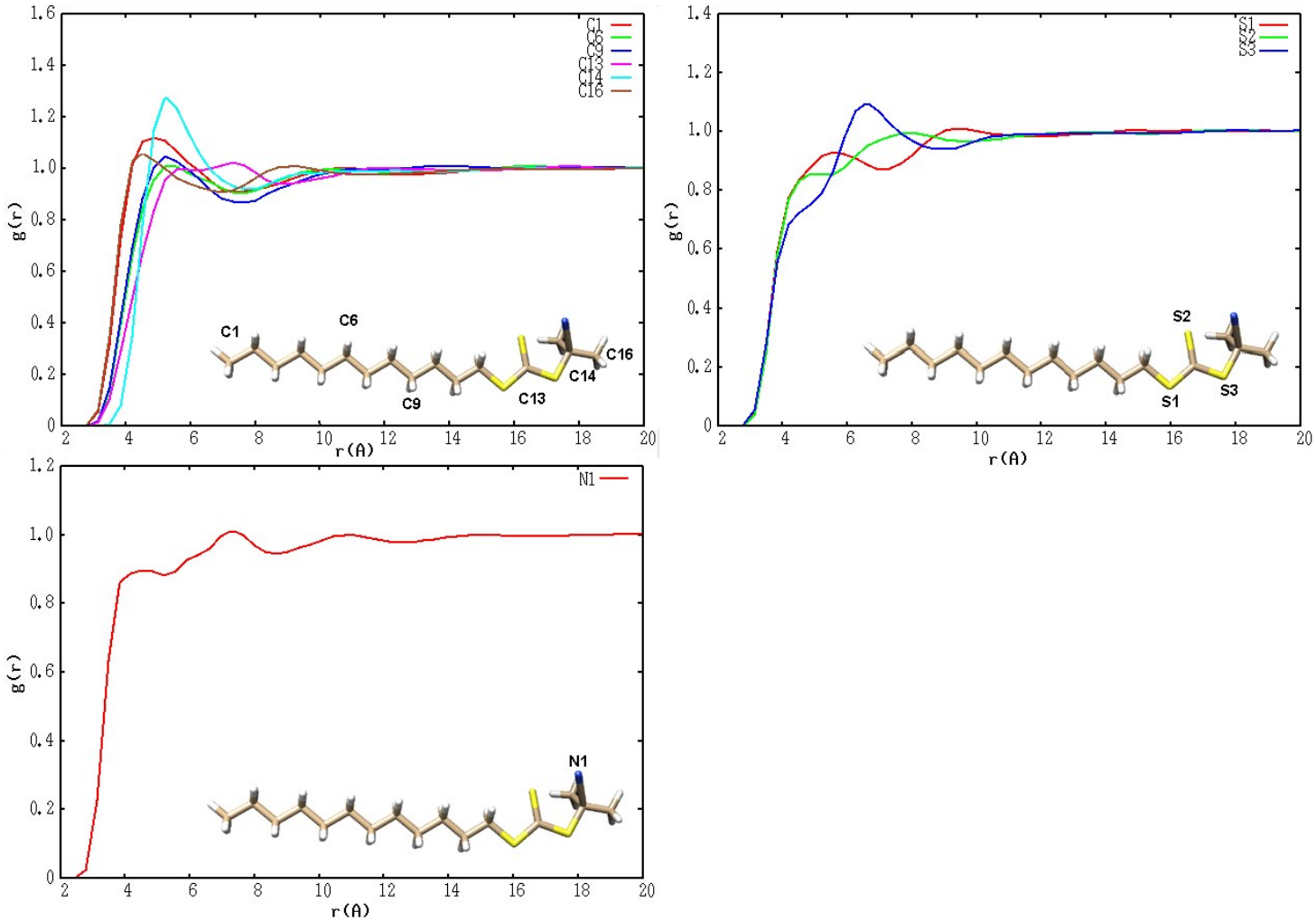

Figure S17 *Radial distribution functions showing the functional groups interactions with toluene, gij(r) (i = O1 - - -, O2 .... or N1 ___ and j = carbon atoms of toluene) vs. interatomic distances. From top left to bottom left: Carbon atoms of CPDT; Sulfur atoms of CPDT; Oxygen atoms of CPDT; and Nitrogen atom of CPDT.*

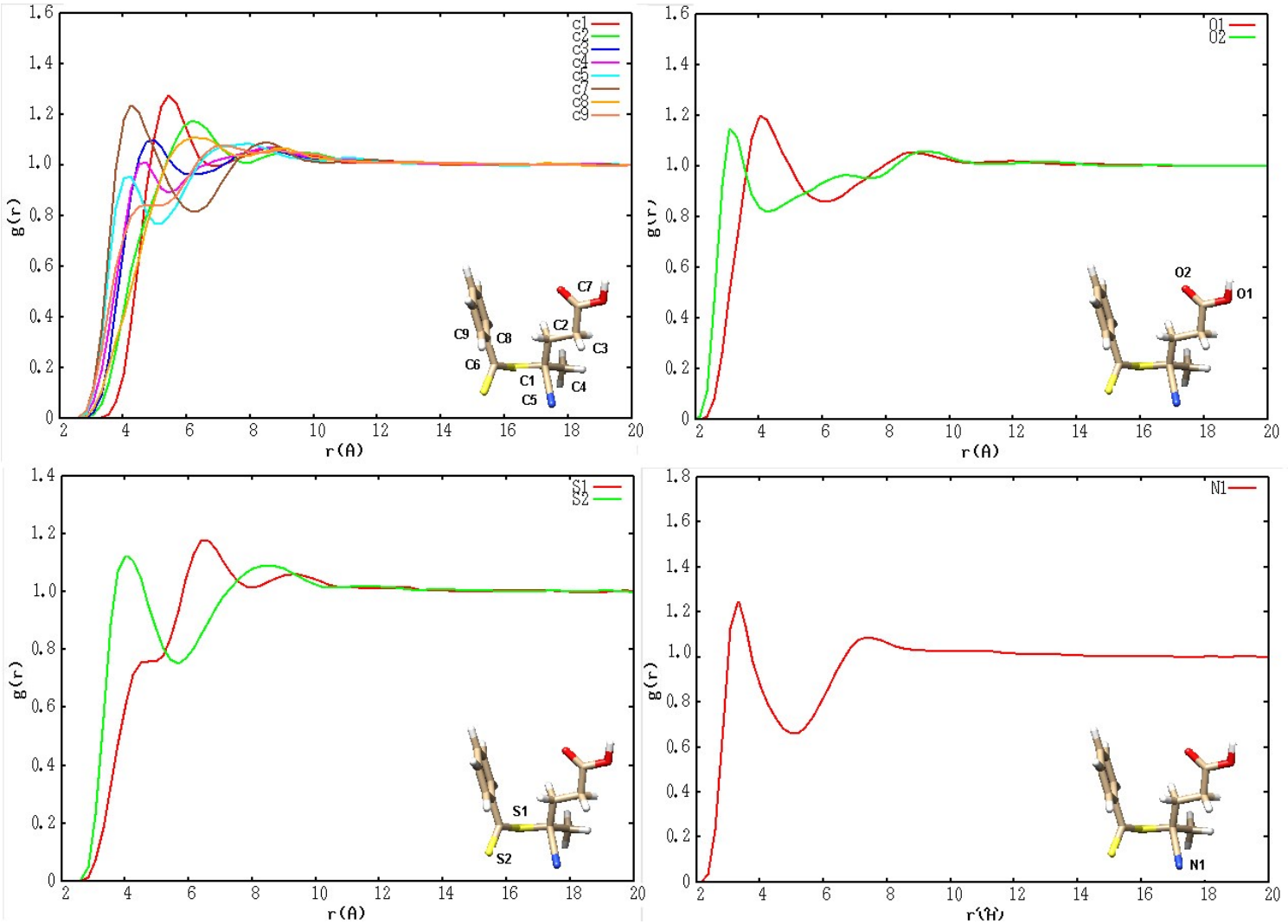

Figure S18 *Radial distribution functions showing the functional groups interactions with $scCO_2$, gij(r) (i = O1 - - -, O2 .... or N1 ___ and j = carbon atoms of CO_2) vs. interatomic distances. From top left to bottom left: Carbon atoms of CPAB; Oxygen atoms of CPAB; Sulfur atoms of CPAB; and Nitrogen atom of CPAB.*

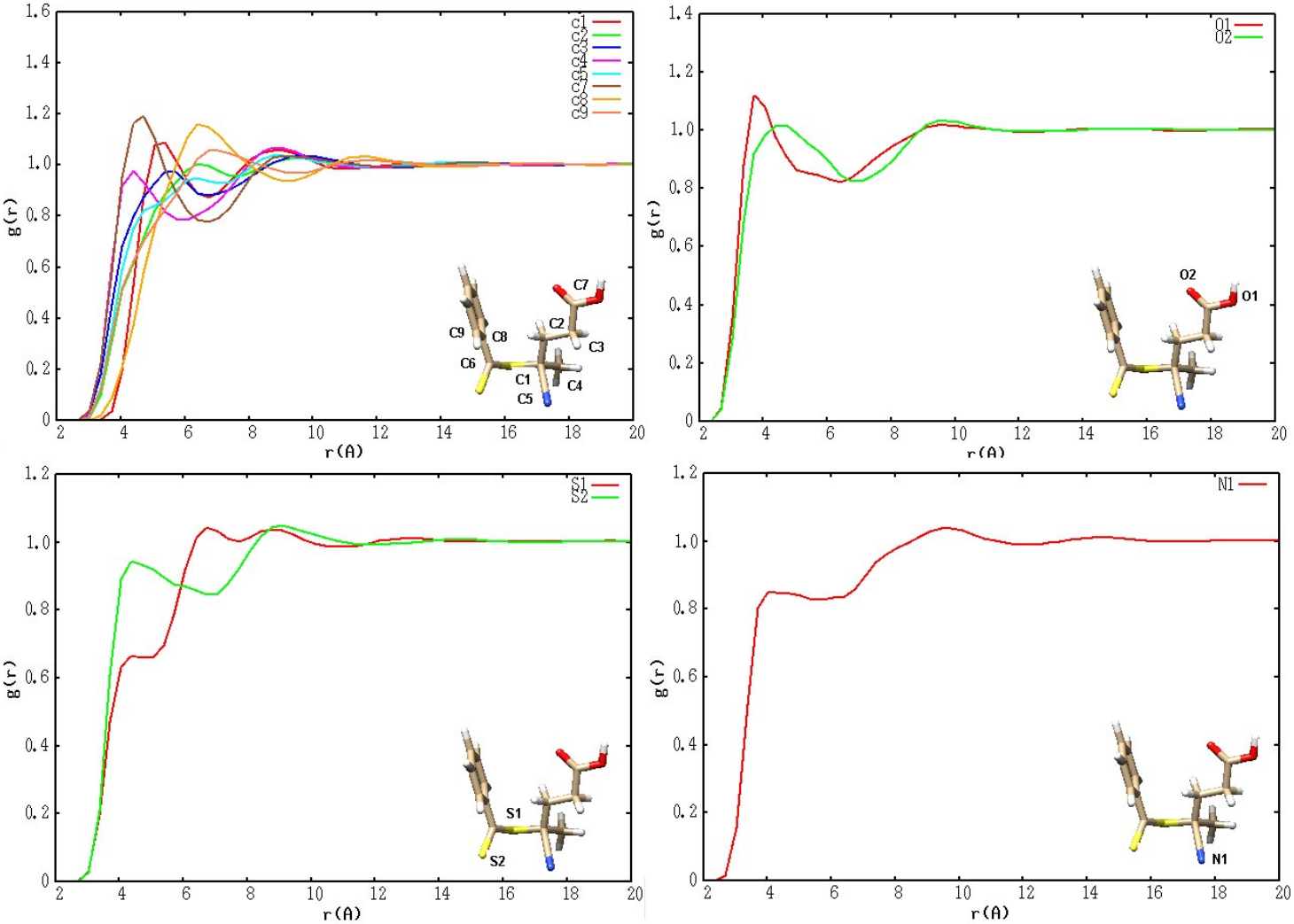

Figure S19 *Radial distribution functions showing the functional groups interactions with toluene, gij(r) (i = O1 - - -, O2 .... or N1 ___ and j = carbon atoms of toluene) vs. interatomic distances. From top left to bottom left: Carbon atoms of CPAB; Oxygen atoms of CPAB; Sulfur atoms of CPAB; and Nitrogen atom of CPAB.*

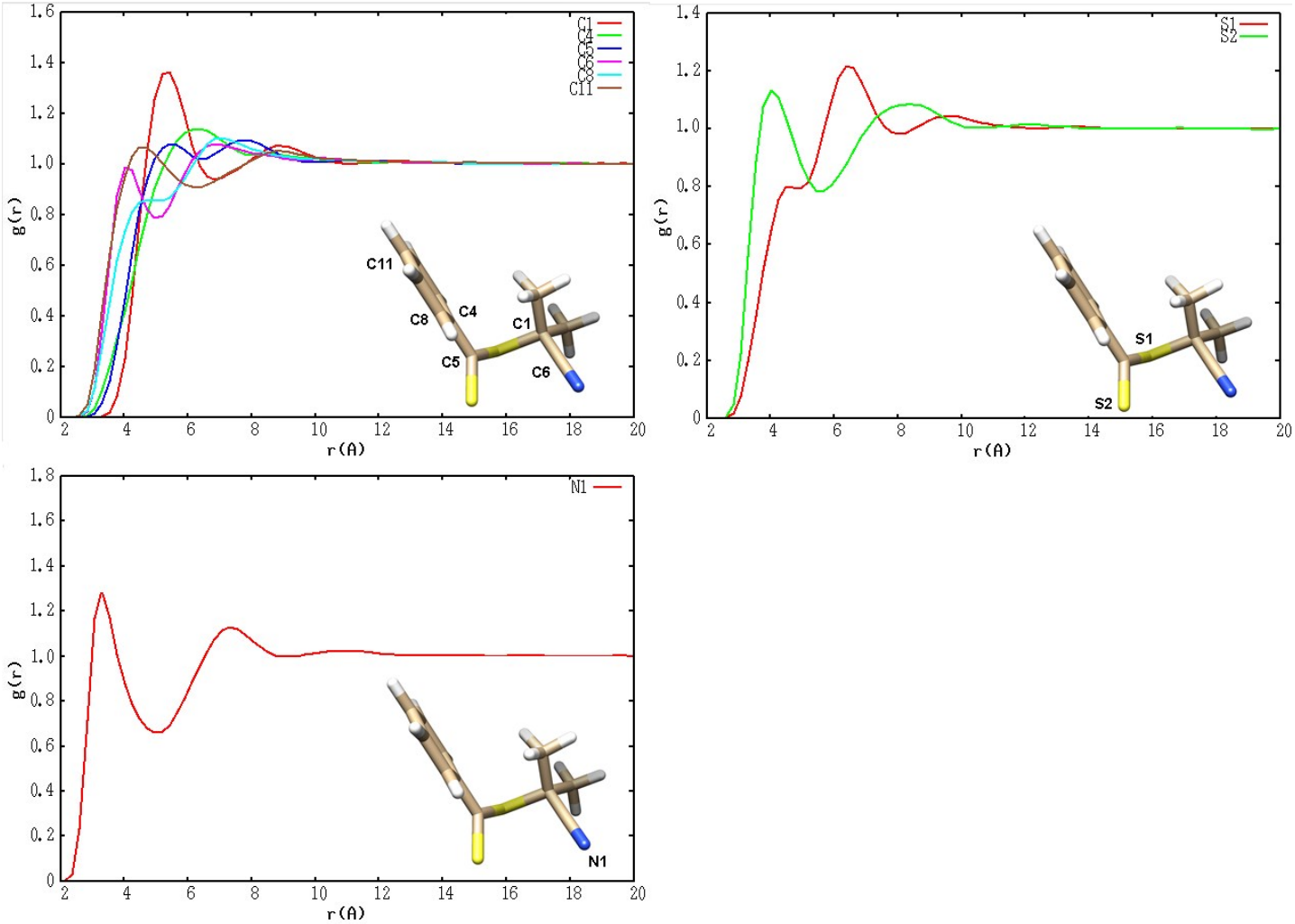

Figure S20 *Radial distribution functions showing the functional groups interactions with $scCO_2$, gij(r) (i = O1 - - -, O2 .... or N1 ___ and j = carbon atoms of CO_2) vs. interatomic distances. From top left to bottom left: Carbon atoms of CPDB; Sulfur atoms of CPDB; and Nitrogen atom of CPDB.*

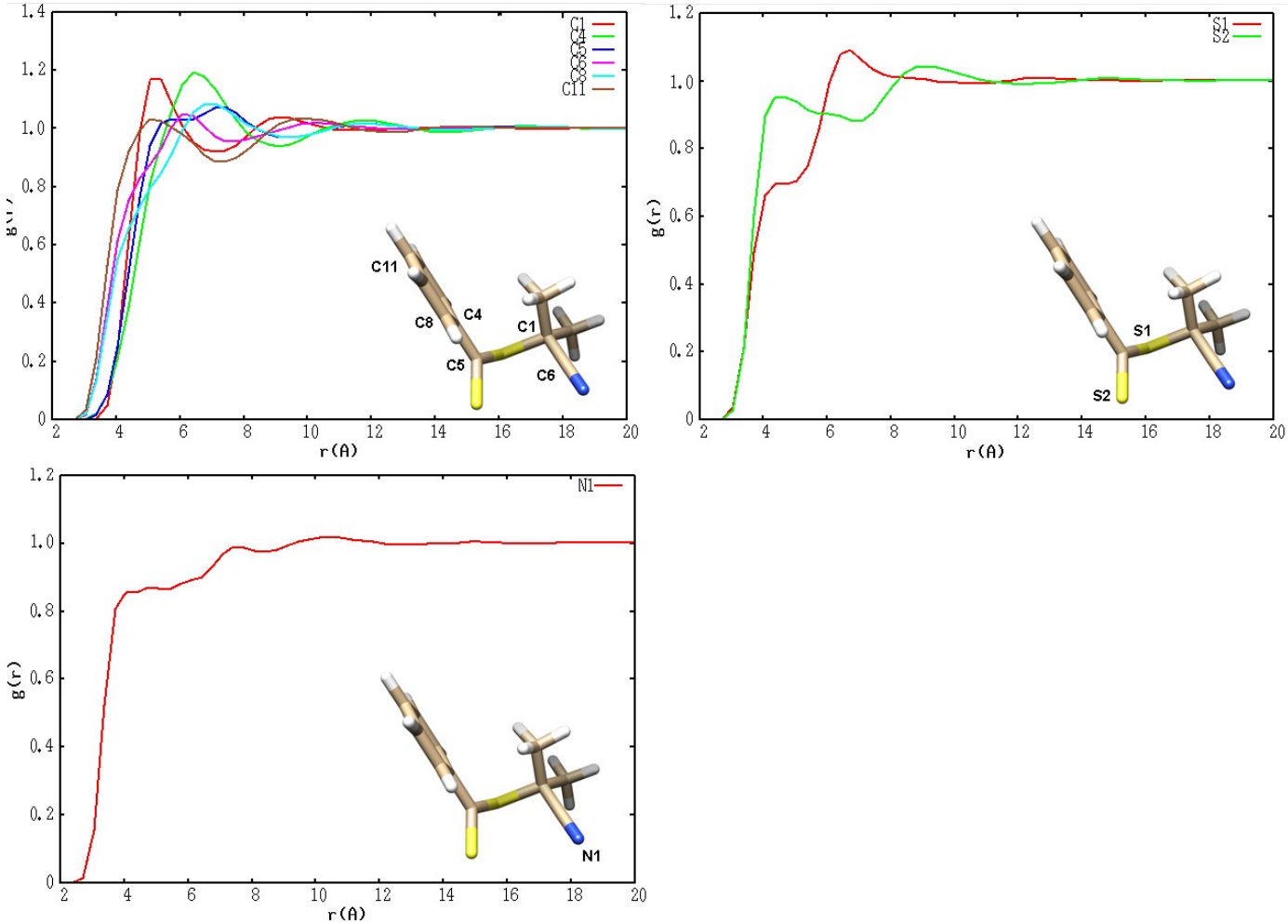

Figure S21 *Radial distribution functions showing the functional groups interactions with toluene, gij(r) (i = O1 - - -, O2 .... or N1 ___ and j = carbon atoms of toluene) vs. interatomic distances. From top left to bottom left: Carbon atoms of CPDB; Sulfur atoms of CPDB; and Nitrogen atom of CPDB.*

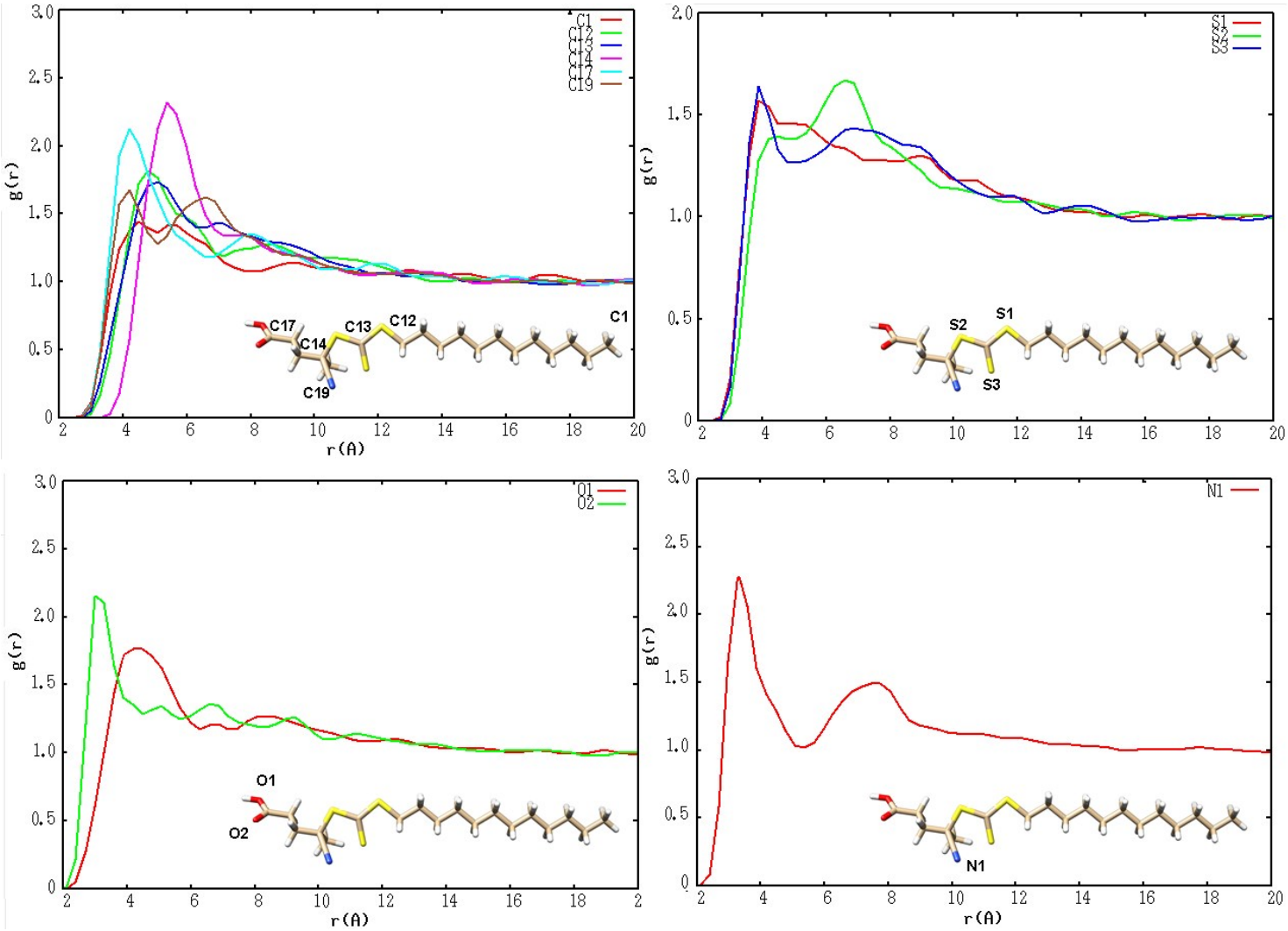

Figure S22 *Radial distribution functions showing the functional groups interactions with $scCO_2$, gij(r) (i = O1 - - -, O2 .... or N1 ___ and j = carbon atoms of CO_2) vs. interatomic distances. From top left to bottom left: Carbon atoms of CPAD; Sulfur atoms of CPAD; Oxygen atoms of CPAD; and Nitrogen atom of CPAD.*

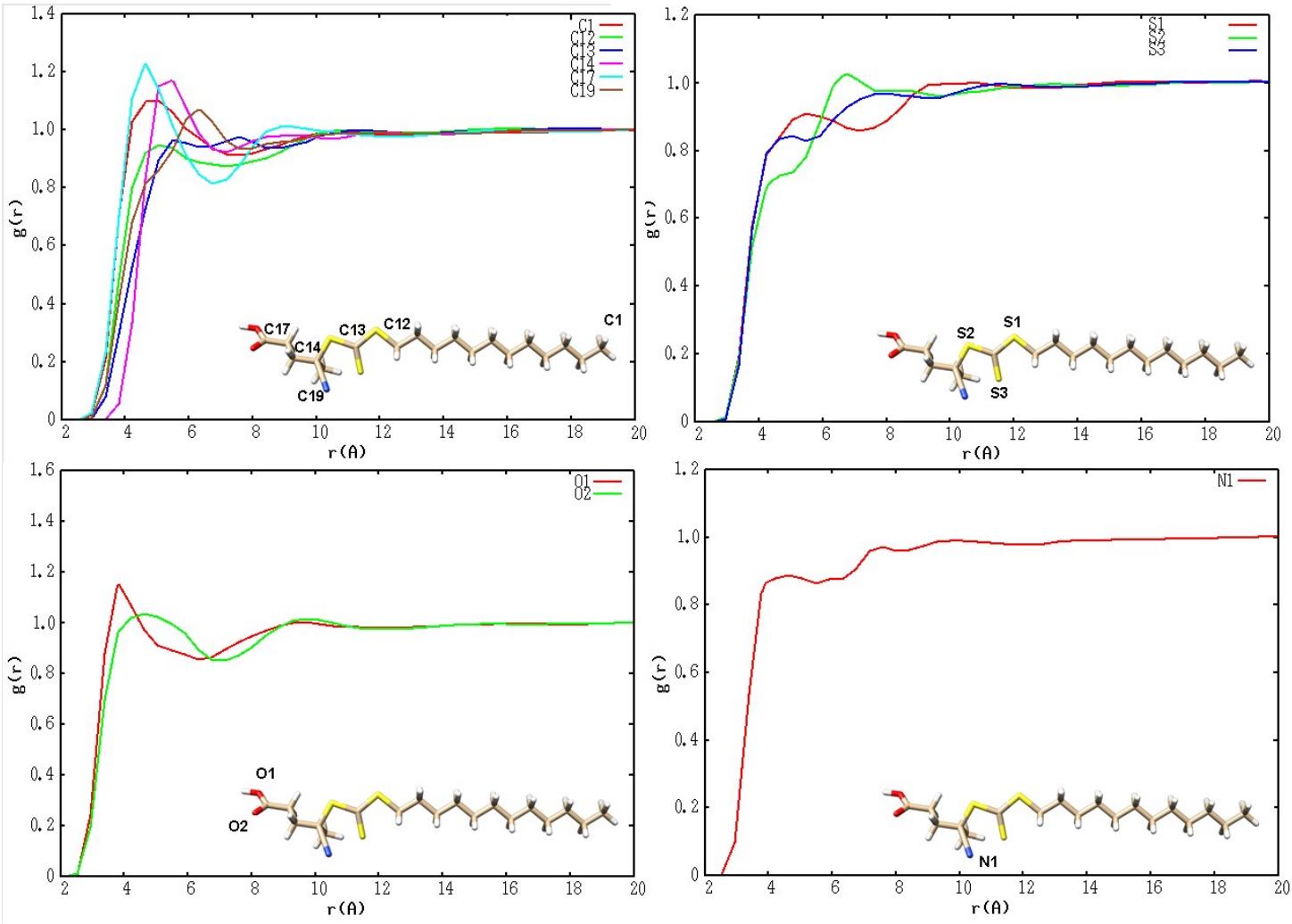

Figure S23 *Radial distribution functions showing the functional groups interactions with toluene, gij(r) (i = O1 - - -, O2 .... or N1 ___ and j = carbon atoms of toluene) vs. interatomic distances. From top left to bottom left: Carbon atoms of CPAD; Sulfur atoms of CPAD; Oxygen atoms of CPAD; and Nitrogen atom of CPAD.*

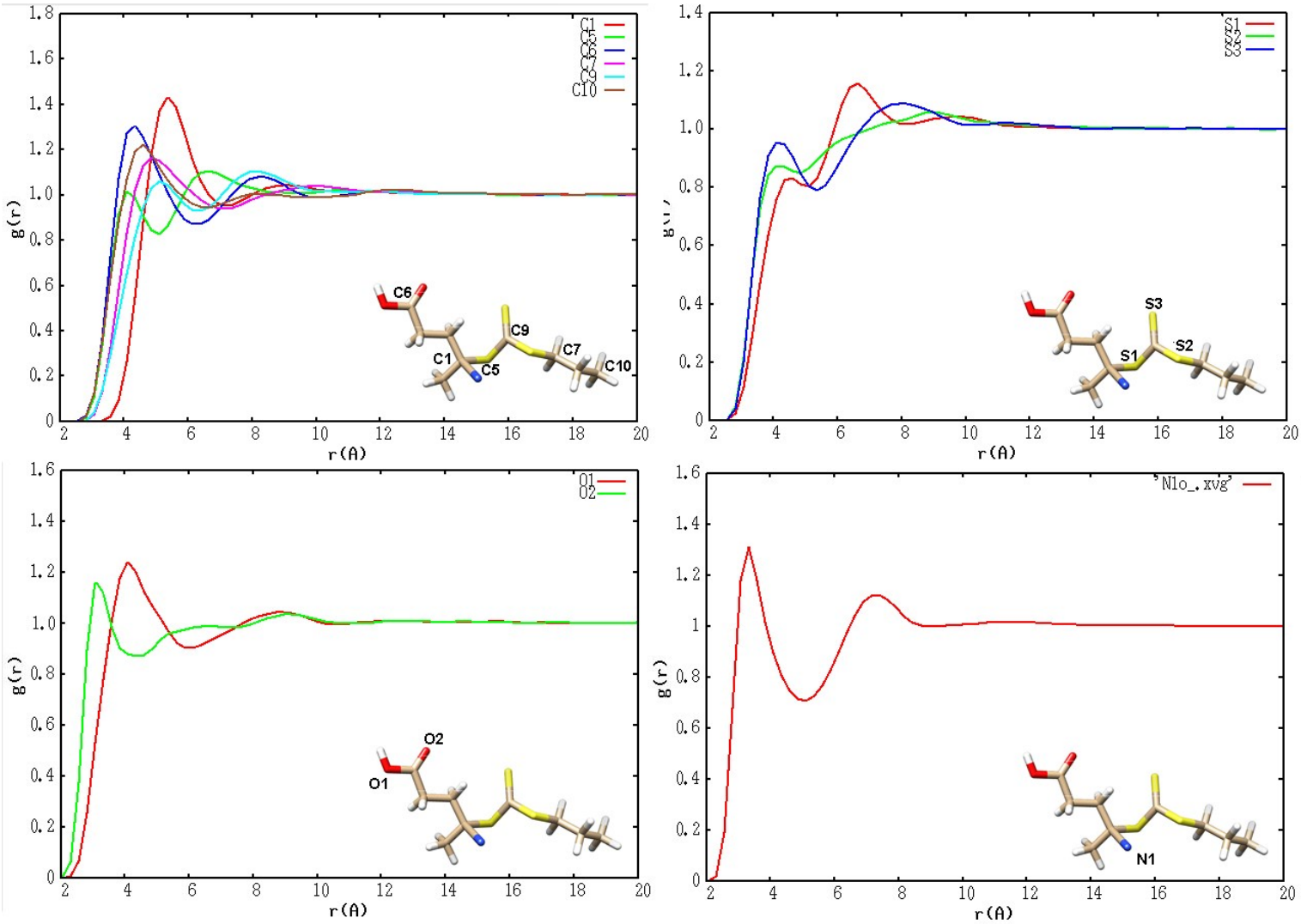

Figure S24 *Radial distribution functions showing the functional groups interactions with $scCO_2$, gij(r) (i = O1 - - -, O2 .... or N1 ___ and j = carbon atoms of CO_2) vs. interatomic distances. From top left to bottom left: Carbon atoms of CTPPA; Sulfur atoms of CTPPA; Oxygen atoms of CTPPA; and Nitrogen atom of CTPPA.*

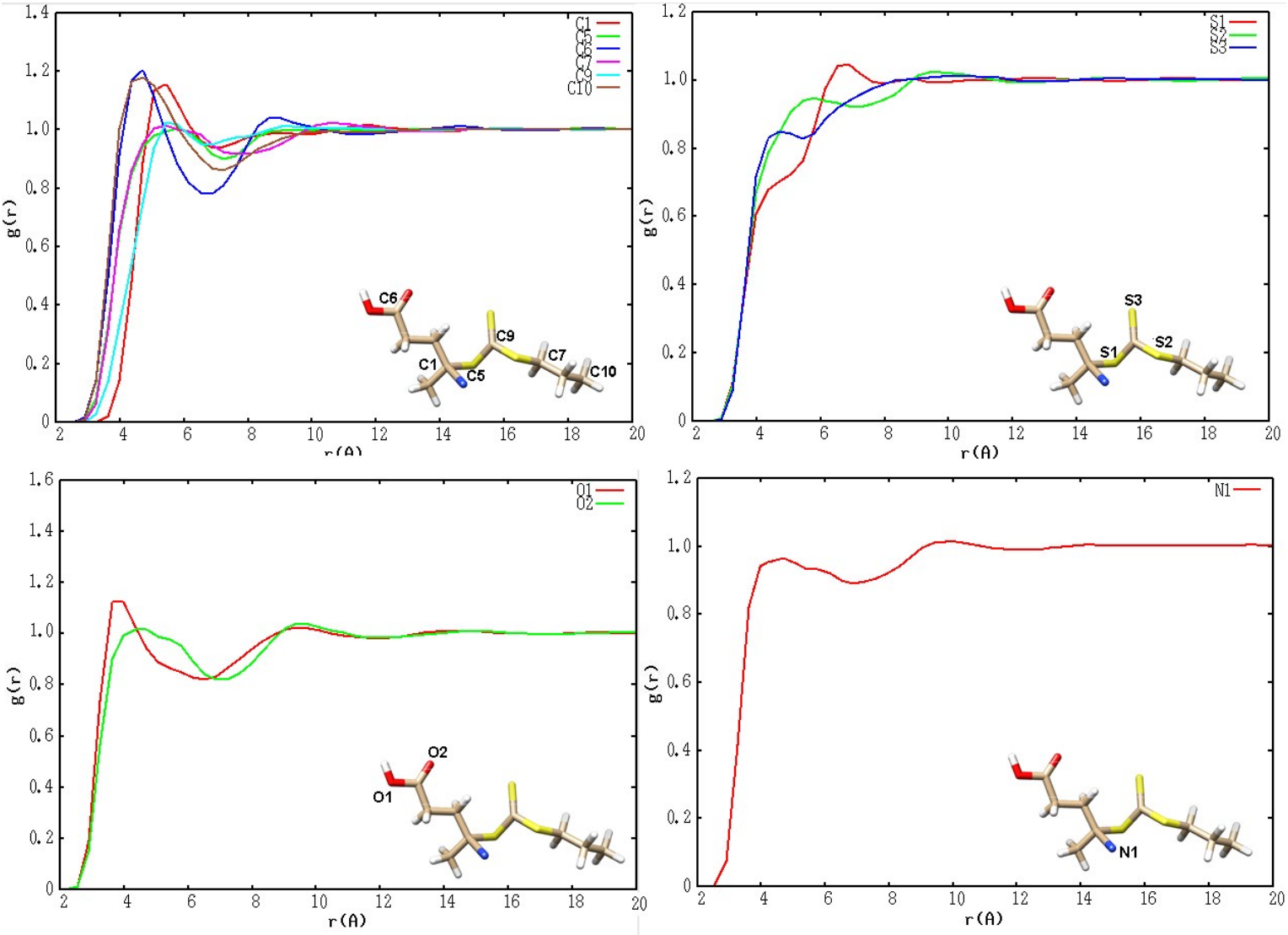

Figure S25 *Radial distribution functions showing the functional groups interactions with toluene, gij(r) (i = O1 - - -, O2 .... or N1 ___ and j = carbon atoms of toluene) vs. interatomic distances. From top left to bottom left: Carbon atoms of CTPPA; Sulfur atoms of CTPPA; Oxygen atoms of CTPPA; and Nitrogen atom of CTPPA.*

References

1. Kortsen, K., et al., *On-line polymerisation monitoring in scCO2: a reliable and inexpensive sampling method in high pressure applications.* J Supercrit Fluids, 2020: p. 105047.